

NEW RESULTS IN TURBULENCE HEATING OF A PLASMA

M. V. BABYKIN, P. P. GAVRIN, E. K. ZAVOĬSKIĬ, L. I. RUDAKOV, V. A. SKORYUPIN, and G. V. SHOLIN

Submitted to JETP editor August 13, 1963

J. Exptl. Theoret. Phys. (U.S.S.R.) 46, 511-530 (February, 1964)

We present the results of new experiments on turbulence heating of a plasma; a theory for the effect has also been developed. In the density range from 10^{12} to 10^{13} cm^{-3} the electron pressure of the plasma is found to be 10^{15} $\text{eV}\cdot\text{cm}^{-3}$, which is approximately 20% of $H_{\sim}^2/8\pi$. Under certain conditions the electron heating is accompanied by heating of the ions to approximately 150 eV. The containment time for ions with temperatures of approximately 100 eV is roughly 130 μsec ; for electrons at a temperature of 500 eV this time is approximately 60 μsec . No strong instabilities are observed during the time in which the plasma is confined. Ion cyclotron waves and characteristic oscillations of the plasma column have been observed.

INTRODUCTION

THE first experimental results on turbulence heating of a plasma in a rapidly varying magnetic field have been reported.^[1-4] In this phase of the work it was possible to establish the dependence of the electromagnetic energy absorbed by the plasma on the strengths of the fixed and variable magnetic fields and it was shown that the absorption could not be attributed to collisional dissipation; several methods of estimating the electron temperature were described. The theory of the effect was considered in detail for conditions in which turbulence heating effects would be expected and a qualitative theoretical estimate of the final plasma temperature was given.

In the present work we report on the results of experiments carried out with a new apparatus whose parameters are such that the plasma electrons can be heated to 1.5 keV; it is also possible to investigate plasma containment in a magnetic trap and to produce collisionless heating of ions in conjunction with the turbulence heating of the electrons.

1. DESCRIPTION OF THE EXPERIMENTAL APPARATUS

A schematic diagram of the experimental apparatus is shown in Fig. 1. The system consists of a glass vacuum chamber 1 (inner diameter 12 cm) which is approximately 2 m in length; at the center there is a single-turn radio-frequency tank coil 2 which is 90 cm in width. The circuit capacity is charged to 100-120 kV and discharged

through a controlled spark gap. The natural frequency of the circuit is 9 Mc/sec and the peak alternating magnetic field H_{\sim} is approximately 500 Oe. The initial chamber vacuum is 5×10^{-6} mm Hg. The vacuum chamber and rf circuit are located in a fixed magnetic field that can be varied from 0 to 3000 Oe; this field is produced by coil 3. The additional coils 4 produce a magnetic-mirror configuration. The mirror ratio can be varied from 1.5 to 3.5. Before the rf circuit is energized a cold plasma is produced in the chamber by means of the plasma injector 5, which is located at one end of the vacuum chamber. The injector consists of an assembly of hydrogen-saturated titanium buttons between which a dis-

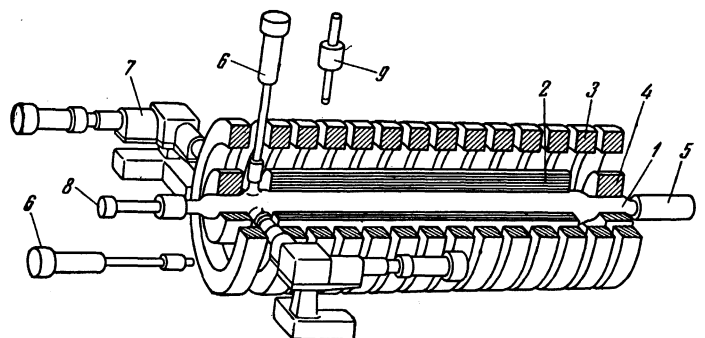


FIG. 1. Diagram of the experimental apparatus: 1) vacuum chamber, 2) rf circuit, 3) coil for producing fixed magnetic field, 4) mirror coils, 5) plasma injector 6) x-radiation detector, 7) monochromator with FÉU-19 photomultiplier, 8) probe connected to electrostatic particle energy analyzer, 9) probe for observation of transverse ion velocities (this can be used in place of 6 which is oriented vertically). The device 6 located horizontally can be introduced into the vacuum chamber in place of probe 8.

charge is produced using a capacity of $0.2 \mu\text{F}$ charged to voltages ranging from 3 to 15 kV. The discharge period is $1.5 \mu\text{sec}$. The discharge circuit contains a resistance of 0.5Ω which is used to damp the oscillations of the discharge current. The total time of operation of the injector is 3–4 μsec . The charged particle density n can be varied from 2×10^{11} to $4 \times 10^{13} \text{ cm}^{-3}$. The density is estimated by cutoff of microwave signals at 10, 3 and 0.8 cm and by the neutral atom ionization time, which is measured by the reduction in the emission of spectral lines.

The electron energy at densities $\sim 2 \times 10^{11} \text{ cm}^{-3}$ is determined by measuring the hardness of the electron bremsstrahlung in thin carbon sheets 6 located in front of a CsI(Tl) crystal in the vacuum chamber. At higher densities the electron temperature is determined by simultaneous observation of the emission lines $\text{H}\beta$ and He I 5875 Å or He I 5016 Å by means of two monochromators 7 provided with FÉU-19 photomultipliers.

The longitudinal velocities of the ions and electrons are measured by means of a probe 8 in conjunction with electrostatic analysis of the particle energy.^[5] The transverse ion velocities are measured by means of probe 9 which is located in the vacuum chamber between the mirror and the rf circuit.

The timing of the operation of the oscilloscopes, plasma injector, and rf circuit is controlled by a synchronization system. The trigger for the rf circuit can be delayed by times ranging from 0 to 100 μsec with respect to the injector trigger.

2. MEASUREMENT OF ELECTRON TEMPERATURE AND DENSITY IN TURBULENCE HEATING OF THE PLASMA

The electron temperature in the plasma has been measured by three methods: (a) by absorption of the electron bremsstrahlung in a thin carbon sheet, (b) by determining the ratio of the quenching rates for various spectral lines, and (c) by means of a probe in conjunction with electrostatic analysis of the particle energies. The bremsstrahlung method can only be used at temperatures greater than 1 keV. The optical method is effective at temperatures below 500 eV. The probe technique is more or less universal. Used together these three methods allow us to determine the plasma electron temperature over a wide range of various experimental parameters. The optical measurements also provide a determination of plasma density in the range 10^{12} – 4

$\times 10^{13} \text{ cm}^{-3}$. Used in conjunction with the microwave measurements these give reliable information on plasma density under various conditions.

A. Measurement of Electron Energy from Bremsstrahlung

It has already been shown in the early work on this subject^[1–3] that the turbulence heating method provides electron temperatures of the order of 1 keV and higher. In the present experiments an attempt was made to observe electron bremsstrahlung in the vicinity of 1 keV. For this purpose, a CsI(Tl) crystal 5 mm in diameter shielded from the plasma light by a thin opaque carbon sheet is placed directly in the vacuum chamber. The crystallographic plane can be parallel or transverse to the magnetic field. The density of the carbon film placed directly against the crystal is 0.4 mg/cm^2 . The plasma electrons striking the film are stopped in a very thin surface layer. The energy of these electrons is converted into x-ray bremsstrahlung which, after partial absorption in the sheet, strikes the crystal, causing a light flash.

In front of the crystal there is a ‘‘flag’’ which is used to introduce absorbers of different thickness or to shield the crystal with a transparent Plexiglas plate 1 mm in thickness without breaking the vacuum. The first experiments at densities of $2 \times 10^{11} \text{ cm}^{-3}$ indicated intense emission from the crystal which could be observed by eye even in an illuminated room. Covering the crystal with a thicker carbon sheet or with a transparent Plexiglas plate causes the emission to disappear completely. Under the present conditions the bremsstrahlung from the plasma volume should be quite small. By placing the crystal parallel to the magnetic field and locating it at various transverse positions in the plasma we have shown that the bremsstrahlung does not come from the chamber walls, but is produced by direct incidence of electrons on the carbon sheet.

In order to estimate the bremsstrahlung energy we have taken oscillograms of the emission from a crystal located behind the mirror (transverse to the magnetic field) and covered by carbon sheets of different thickness. The light from the crystal reaches the FÉU-19 photomultiplier located outside the magnetic field by means of a light pipe. The photocathode of the FÉU is covered by a diaphragm with an aperture 3.5 mm in diameter because the light intensity is so high that the photomultiplier is overloaded. The signal from the photomultiplier is then fed to the amplifier of an OK-17 oscilloscope.

In Fig. 2a we show oscillograms of FÉU signals for various absorber thicknesses. The emission appears immediately after the rf circuit is energized. The sharp reduction in emission with time is due to the rapid rf heating of the plasma: this means that the first electrons to be lost from the trap are those with velocities lying within the escape cone. After these electrons are lost the loss of plasma through the mirrors is determined by particle collisions, a process that gives an appreciably smaller loss flux.

These oscillograms can be used to determine the electron temperature if the electron energy distribution is known. If a Maxwellian distribution is assumed the experimental results correspond to a temperature $T_e \approx 1.5$ keV. Approximately the same temperature value is obtained with a rectangular distribution of width T_e or with a Druyvesteyn distribution. The exact form of the distribution function is not known at densities $2 \times 10^{11} \text{ cm}^{-3}$. However, probe measurements at $n = 10^{12} \text{ cm}^{-3}$ and a temperature of 500 eV indicate that the electron energy distribution is smooth and that it has a single peak in the region of the mean energy value. Thus it may be assumed that the figure given above represents a reliable estimate of electron temperature.

In Fig. 2b we present the results of temperature estimates obtained by interpreting the oscillograms for various instants of time. Unfortunately, with the sensitivity that was used it is not possible to estimate the temperature at times greater than 10 μsec ; the limitation on sensitivity arises because the photomultiplier is overloaded at the beginning of the pulse at higher sensitivities and the oscillograms become highly distorted.

B. Optical Measurements of Electron Temperature and Density

If the initial electron density is high $\gtrsim 10^{12} \text{ cm}^{-3}$ and if the residual or admitted neutral gas pressure is high it then becomes possible to determine the electron temperature from the emission lifetime of two spectral lines. In the absence of thermodynamic equilibrium the line intensity is given by

$$I_\lambda \sim \frac{hc}{\lambda} n_e \langle v_e \sigma(v_e) \rangle n_\alpha(t)$$

and depends on the instantaneous value of the density n_α of atoms of a given kind α and on the mean rate of excitation of the emitted line $n_e(t) \langle v_e \sigma(v_e) \rangle$, where the angle brackets denote averages over the electron distribution function.

At electron densities of approximately $\sim 10^{12} \text{ cm}^{-3}$ and higher the emission intensity is sufficient for detection at gas pressures up to $5 \times 10^{-6} \text{ mm Hg}$ ($n_\alpha \sim 2 \times 10^{11} \text{ cm}^{-3}$). It is then possible to study the plasma emission in separate spectral lines with a rather low neutral density, in which case the contributions due to secondary electrons and atomic excitation and ionization can be neglected. When the mirrors are turned on the density of electrons capable of ionization then remains essentially the same and the line intensity becomes a function of the electron temperature alone. The initial value of the temperature can be established by comparing the computed and experimental intensity of the spectral lines as functions of time. This analysis is simplified considerably at temperatures greater than 40–50 eV because the temperature change due to loss of electrons by virtue of excitation and ionization of neutrals is never greater than 20–30%. Thus, during this time interval the line intensity falls off exponentially with the atom concentration. The decay time for the line is then equal to the time required for ionization of atoms of a given kind $1/n_e \langle v_e \sigma_{\text{ion}} \rangle$ and can be easily related to the electron temperature. Obviously this statement holds only when there is no strong influx of impurities into the plasma during the time interval being investigated. Recent spectroscopic investigations (cf. [6]) have shown that in turbulence heating the influx of impurities and the impurity contribution in the energy balance are both negligibly small.

If two gases are used (in the present experiments, hydrogen and helium) the optical measurements of the variation of density with time make possible a simultaneous determination of the temperature and density of the electrons. For this purpose it is only necessary to know the value of

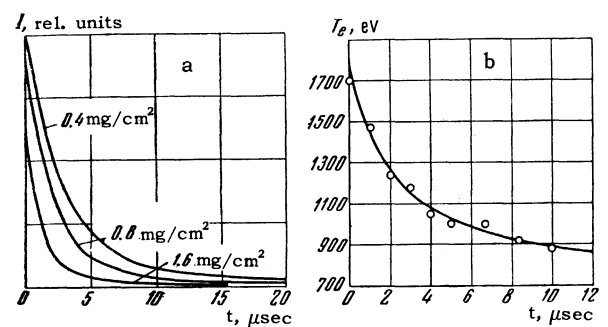


FIG. 2. a) Oscillograms of the emission from the CsI(Tl) crystal for electron bremsstrahlung in carbon sheets of different thickness; b) the electron temperature as a function of time determined from these oscillograms.

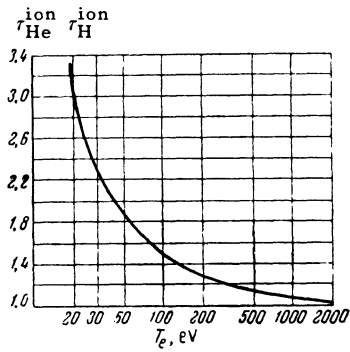


FIG. 3. Theoretical curve for the ratio of the e-folding times for the He I 5875 Å and the H β line as a function of electron temperature T_e . The calculations are carried out assuming a Maxwellian electron distribution. The curve is used to determine T_e in the range between 30 and 500 eV.

the averaged quantity $\langle v\sigma_{\alpha}^{\text{ion}} \rangle$ as a function of temperature for each atomic species. The ratio of the ionization times can be used to determine the electron temperature (cf. Fig. 3); then, using the ionization lifetime and the electron temperature the electron density can be found.

In Fig. 4 we show two pairs of oscillograms of the emission of lines from hydrogen and helium taken in one experiment. From the ratio of the decay time of the emission for these spectral lines one determines the plasma temperature using the curve in Fig. 3. The first pair corresponds to $T_e = 40$ eV, $n_e = 3 \times 10^{13}$ cm $^{-3}$ while the second corresponds to $T_e = 200$ eV, $n_e = 6 \times 10^{12}$ cm $^{-3}$. To use this method it is necessary to know the quantity $\langle v\sigma_{\alpha}^{\text{ion}} \rangle$ which, in gen-

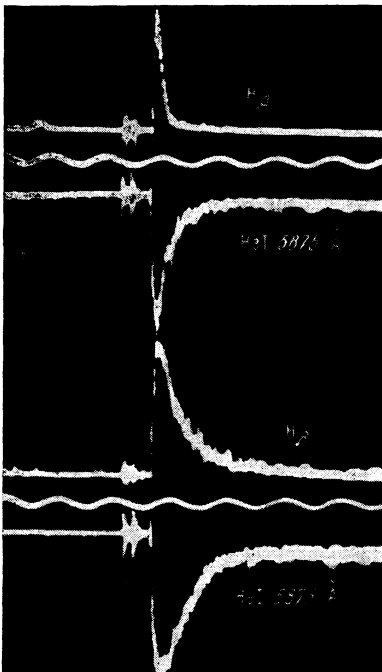


FIG. 4. Oscillograms of the emission of the H β and He I 5875 Å lines for turbulence heating of a plasma in a trap taken in one experiment. The neutral atoms of hydrogen and helium amount to less than 10% of n . The period of the sine wave is 10 μ sec.

eral, depends on the choice of the distribution function. This dependence, however, is very weak and the method should give reasonably reliable results in the region $30 \text{ eV} < T_e < 500 \text{ eV}$. At lower temperatures the electron loss becomes important and at higher temperature the ratio $\langle v\sigma_{\text{H}}^{\text{ion}} \rangle / \langle v\sigma_{\text{He}}^{\text{ion}} \rangle$ becomes essentially constant.

The results of optical measurements of electron temperature and density are shown in Fig. 17 (cf. below).

C. Probe Measurements of the Electron Temperature

The velocity distributions of the electrons and ions in the direction of the magnetic field has been measured by using a probe in conjunction with an electrostatic analysis of the particle energy.^[5] The probe is placed in the vacuum chamber behind the mirror in order to avoid perturbing the plasma. This probe is a grounded metal cylinder 34 mm in diameter whose end face is covered with a copper foil having 50 apertures 0.1 mm in diameter. To the first grid of this probe is applied a separation potential which retards charged particles of one sign and extracts particles of the other; these extracted particles are then energy-analyzed by an analyzing potential applied to a second grid. A third grid located in front of the collector is grounded.

In order to verify the probe accuracy we investigated the energy distribution of the ions in plasmoids produced by the plasma injector (Fig. 5). The negative separation potential was 550 V and the mean energy of the directed motion of ions from the plasma injector was found to be 90 eV, in good agreement with the ion energy as measured by the time of flight.

A positive separation potential is used to study the electron energy distribution and the retarding voltage on the analyzing grid is varied from 0 to 1500 V. As in the bremsstrahlung measurement

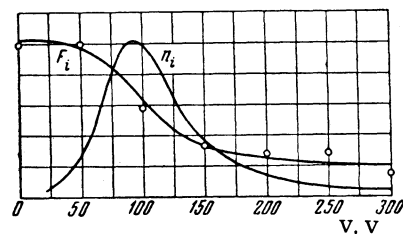
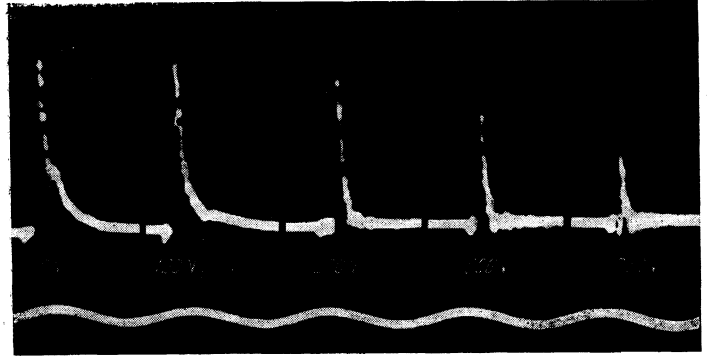


FIG. 5. The probe current (F_i , relative units) for different retarding potentials V and the ion distribution (n_i , relative units) from the plasma injector as functions of the energy of directed motion; $H = 500$ Oe. The voltage to the condenser bank is 13 kV.

FIG. 6. Oscillograms of the electron current to the probe after turbulence heating of the plasma for various analyzing potentials. The period of the sine wave is $10 \mu\text{sec}$.



the signal is produced primarily by electrons which acquire velocities lying in the escape cone as a result of heating. Thus, the duration of the current pulse is not determined by the lifetime of the hot plasma but by the time required for these electrons to escape from the trap. It is not possible to increase the sensitivity of the probe in order to analyze electrons escaping from the trap by virtue of collisions because of the overloading of the amplifier due to the first pulse. The flux of electrons escaping from the trap as a consequence of collisions is considerably weaker and is not recorded in the present experiments.

In Fig. 6 we show typical oscillograms of electron current at the initial time with various retarding potentials. Using these oscillograms one can find the electron energy distribution for various values of the fixed and alternating magnetic fields and for different plasma densities. A typical curve showing the electron energy distribution is shown in Fig. 7. A peak is observed near 500 eV. These probe measurements are in good agreement with the optical measurements (cf. below, Fig. 17). No noticeable effect of secondary emission on the energy measurements was observed up to 500 eV for the ions and up to 150 eV for the electrons. This result was established in special control experiments.

In Fig. 8 we show the electron temperature as

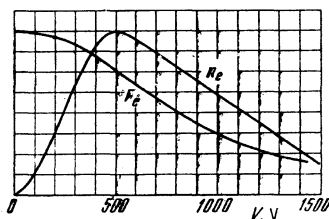


FIG. 7. The electron current to the probe (F_e , relative units) as a function of the analyzing potential of the probe and the electron energy distribution in turbulence heating ($n_e = dF_e/dV$ is the number of electrons having a given energy in relative units), $H_- = 500 \text{ Oe}$, $H = 400 \text{ Oe}$, initial plasma density $n_e = 2 \times 10^{12} \text{ cm}^{-3}$.

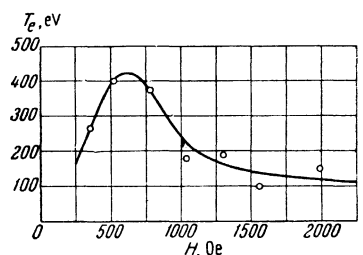
a function of the fixed magnetic field. The maximum temperature is obtained at fixed fields of approximately 600 Oe; at higher fields (up to 2000 Oe) the electrons are still heated to temperatures of 100–150 eV. This dependence of electron temperature on field is in agreement with the behavior of the energy absorption from the rf circuit obtained earlier.^[2]

3. TURBULENCE HEATING OF IONS

It was established with the apparatus described in [3,4] that the ions are heated at fixed magnetic fields greater than 1000 Oe; this effect could not be attributed to the collisions of plasmoids that were studied in this work. This phenomenon was detected by means of the probe described in [4]. The dependence of ion temperature on magnetic field obtained under these conditions is shown in Fig. 9a. Although simultaneous measurements of the dependence of electron and ion temperatures on field were not made it appears that the maximum ion heating occurs at high fields, where the electron heating has already been reduced. As the strength of the alternating magnetic field is increased the peak is displaced in the direction of higher fixed fields (Fig. 9b). These observations were the motivation for building the new apparatus with increased tube diameter that could contain high energy ions.

In the new apparatus the ion heating is observed by means of two probes which are perpendicular and parallel to the magnetic field. The first of

FIG. 8. The electron temperature T_e as a function of the strength of the fixed magnetic field as obtained from probe measurements; $H_- = 500 \text{ Oe}$, $n_e = 2 \times 10^{12} \text{ cm}^{-3}$.



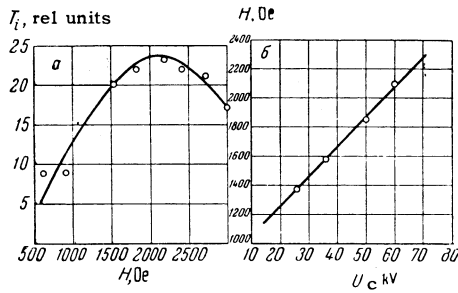


FIG. 9, (a) The ion temperature in turbulence heating as a function of the fixed magnetic field H and (b) the position of the peak in the ion heating curve as a function of the rf circuit voltage U_c (the circuit frequency 1.2×10^7 cps); $H_- = 800$ Oe, $n = 10^{13}$ cm^{-3} .

these is a grounded copper cylinder 100 mm in diameter whose end face is covered by copper foil. The foil contains 100 apertures 0.1 mm in diameter. The probe is introduced into the plasma across the magnetic field. Inside the cylinder there is a collector separated from the input apertures by a distance of 6 mm. Thus, only ions with a Larmor radius greater than this distance can reach the collector. When the magnetic field is changed from 500 to 1500 Oe the threshold energy is changed from 4 to 36 eV correspondingly. The electrons do not reach the collector since the electron Larmor radius at these magnetic fields is much smaller than the distance between electrodes. The probe does not show any readings when a plasmoid is produced by the injector; after the operation of the rf circuit there are strong signals of positive polarity in the absence of any external voltage. This result can be explained only by assuming large transverse velocities for the ions.

A more detailed probe investigation was carried out in conjunction with electrostatic analysis of the longitudinal energy of particles beyond the mirror. In Fig. 10 we show the probe reading as

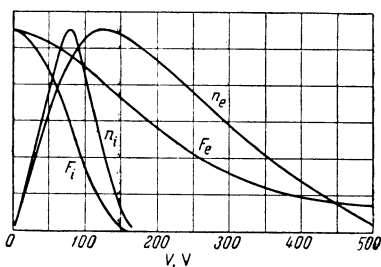
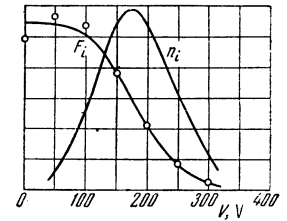


FIG. 10. Probe current for ions (F_i) and electrons (F_e) under the same conditions as functions of the probe analyzing potential; we also give the ion distribution ($n_i = dF_i/dV$) and the electron distribution ($n_e = dF_e/dV$) in energy (same conditions); $H_- = 500$ Oe, $n = (2-3) \times 10^{12}$ cm^{-3} , $H = 1100$ Oe.

FIG. 11. Ion probe current and the ion energy distribution for the case $n = 10^{12}$ cm^{-3} , $H_- = 500$ Oe, $H = 370$ Oe. The peak in the distribution curve lies near 175 eV.



a function of retardation potential and of the energy distributions for the electrons and ions obtained under identical conditions. The peaks of the distributions for the electron and ion energies lie at 130 and at 80 eV respectively. The maximum ion temperature recorded in these experiments was 175 eV (Fig. 11). This result was obtained with an rf circuit voltage of 120 kV.

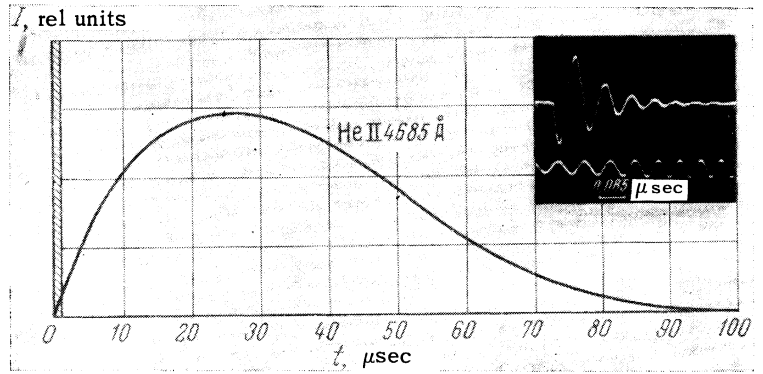
The results given here lead to the conclusion that the turbulence heating method allows simultaneous heating of electrons and ions. In these experiments we have obtained ion temperatures of 100–175 eV with alternating fields of 400–600 Oe. Using alternating fields of higher amplitude would give the possibility of obtaining still hotter plasmas.

4. CONTAINMENT OF A TURBULENCE-HEATED PLASMA

After the turbulence-heating process the time for which the high electron and ion temperatures can be maintained is very sensitive to the presence of the mirrors, although the mirrors have essentially no effect on the heating itself. This result indicates that the plasma is cooled primarily at the ends of the plasma column rather than across the magnetic field.

An idea of the containment time for hot electrons can be obtained, as before,^[2,3] by observing the emission of the He II 4685 Å line (Fig. 12). Helium is added to the hydrogen plasma in amounts less than 10% and is not ionized before the turbulence heating occurs. Hence, after plasma heating the intensity of emission of the He II 4685 Å line grows, serving as a measure of the neutral helium that is ionized; this intensity then diminishes by virtue of the secondary ionization of helium and cooling of the electrons. Using the optical technique described above the electron temperature and plasma density are measured in the same experiments. It is thus possible to compare the measured electron containment time with the calculated time under the assumption that the escape of plasma electrons captured in the trap is due to collisions. The calculation is carried out using the expression

FIG. 12. Intensity of the emission of the He II 4685 Å line after turbulence heating of the plasma. The hatched region indicates the total time the circuit is in operation. The insert in the upper right shows an oscillogram of the current in the circuit; the period of the calibrating sine wave is 0.085 μsec.



$$\tau_e = \sqrt{m} (|\ln \alpha| - 0.6) T^{3/2} / 6.1 \Lambda e^4 n,$$

where e and m are the charge and mass of electron, α is the mirror ratio, and Λ is the Coulomb logarithm. Substituting the measured values $n = 10^{12} \text{ cm}^{-3}$, $T_e = 500 \text{ eV}$ and the mirror ratio $\alpha = 3$, we find $\tau_e = 0.7 \times 10^{-4} \text{ sec}$. This value is approximately the same as the measured value $\tau_e \text{ exp} = 60 \mu\text{sec}$.

In another series of measurements carried out at higher values of the fixed magnetic field, in which case the ions and electrons are heated approximately uniformly, we have studied the containment of hot ions. An idea of the containment of hot ions in the trap can be obtained from the readings of the ion probe located perpendicularly to the magnetic field (cf. Sec. 3).

In Fig. 13 we show typical oscillograms of the probe readings with the mirrors switched on. The oscillograms indicate a long (approximately 130 μsec) containment of heated ions in the trap. Clearly evident are the current oscillations with fundamental close to the ion cyclotron frequency.

In these experiments we also measured the plasma density by optical methods and the ion and electron temperatures by means of probes. The following mean values were obtained:

$$T_i = 10^3 \text{ eV}, \quad T_e = 1.5 \cdot 10^2 \text{ eV}; \quad n = 10^{12} \text{ cm}^{-3}.$$

Thus, the calculated containment times for the ions and electrons in the "probkotron" are $\tau_i = 1.3 \times 10^{-3} \text{ sec}$ and $\tau_e = 1.2 \times 10^{-5} \text{ sec}$. The measured value of τ_i^{exp} is found to be $\sim 1.3 \cdot 10^{-4} \text{ sec}$ so that $\tau_e < \tau_i^{\text{exp}} < \tau_i$.

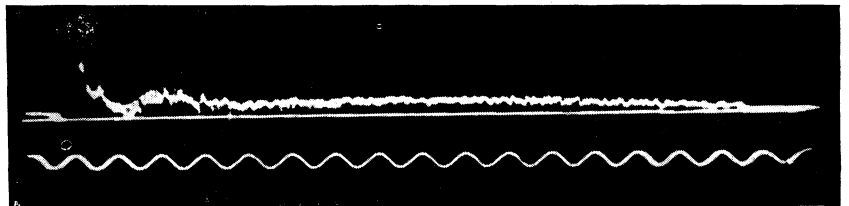
This time relation can be explained as follows.

After a time τ_e the temperature of the plasma electrons is reduced appreciably because of the escape of hot electrons which interact with the end plates of the apparatus, and because of the influx of cold electrons. In this case the plasma density is obviously maintained at the density of hot ions contained in the trap. It may be assumed that the experimentally measured containment time τ_i^{exp} is determined by charge exchange. This assumption is reasonable because atomic hydrogen can enter the trap from the injector. Hydrogen is essentially the only gas on which appreciable charge exchange can occur. Direct experiments show that charge exchange on the residual gas in the chamber is insignificant: the time τ_i does not change as the residual gas pressure is raised from 5×10^{-6} to $3 \times 10^{-5} \text{ mm Hg}$.

Thus, as in the earlier work,^[3] the experimentally measured containment time for the plasma electrons is found to be close to the escape time computed on the basis of collisions. Further evidence that the plasma in the trap is stable in the present experiments is provided by observations of low-frequency noise in the plasma (cf. the following section). The random fluctuations characteristic of a convectively unstable plasma have not been observed.

A possible mechanism for the stabilization of the convective instability in the present experiments has been pointed out in.^[3] As before, we are inclined to believe that the plasma is stable as a consequence of the electric contact with the

FIG. 13. Oscillogram of the ion current to the probe oriented perpendicularly to the fixed magnetic field. The mirror ratio is 3.4 the period of the calibrating sine wave is 10 μsec, $H_z = 500 \text{ Oe}$, $H = 500 \text{ Oe}$, $n = 10^{12} \text{ cm}^{-3}$.



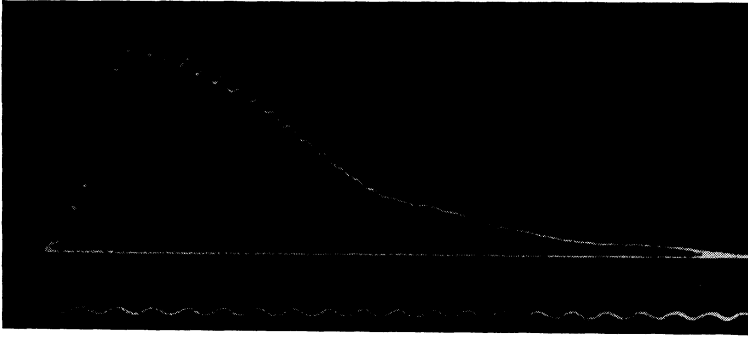


FIG. 14. Oscillogram of the ion current to a probe located between the mirror and the rf circuit perpendicularly to the fixed magnetic field $H = 680$ Oe. The coherent oscillations at a frequency of 0.83 Mc/sec are clearly evident on the oscillogram. The period of the calibrating sine wave is $2.5 \mu\text{sec}$.

metal endplates of the apparatus; this contact is made through the cold plasma which is always available in sufficient amounts beyond the mirrors.

5. LOW FREQUENCY NOISE IN TURBULENCE HEATING OF A PLASMA

The noise in the plasma is observed by means of probe 9 (Fig. 1); the signals from this probe are applied to the input in the amplifier of the OK-17 oscilloscope which has a bandwidth of 10 Mc/sec. The oscillograms of the ion current show strong coherent oscillations (Fig. 14). Sometimes these oscillations are damped and then appear later. These oscillograms show that the fundamental frequency is accompanied by harmonics. In Fig. 15 we show the frequency as a function of fixed magnetic field. On the bases of these data it can be concluded that these are ion-cyclotron oscillations. No other low-frequency oscillations have been observed.

In addition to ion-cyclotron oscillations, under certain conditions turbulence plasma heating seems to excite magnetic sound resonances. The signal from a double electric probe located in the plasma which measures the field E_φ is applied to the plates of an OK-19 oscilloscope. With appropriate choice of density and fixed magnetic field there are oscillations at the frequency of the rf circuit but characterized by a quality factor (Q) appreciably greater than the Q of the circuit itself (Fig. 16a). In some cases these oscillations jump to another mode, as is evident from Fig. 16b. Evidently magnetic-sound oscillations are excited by the rf circuit during the plasma heating period.

6. THEORY AND DISCUSSION OF RESULTS

In formulating a theory for turbulence heating we have started from the assumption that this effect is due to a current-driven instability in the plasma.

The alternating magnetic field H_\sim produced by the rf circuit excites a hydromagnetic (magnetic sound) wave in the plasma that fills the inner volume of the tank coil. The magnetic field gradient in the wave is related to the electron current flowing in the plasma by the expression

$$j = -enu = -\frac{c}{4\pi} \frac{\partial(H_\sim)_z}{\partial r}.$$

If the current density exceeds some critical value $j^* = -enu^*$, where u^* is the critical current-associated velocity of the electrons, which is determined below, the electron stream will excite oscillations at some range of values of k (k and ω_k are the wave vector and oscillation frequency).

The oscillations most likely to be excited are electrostatic oscillations ($\mathbf{E} = -\nabla\varphi$) for which the dispersion relation is [7]

$$\begin{aligned} \varepsilon(\omega, \mathbf{k}) &\equiv 1 - \frac{\omega_{pi}^2}{(\omega + \mathbf{k}\mathbf{u})^2} + \frac{2\pi}{k^2} \omega_{pe}^2 \int_0^\infty v_\perp dv_\perp \cdot \sum_{l=-\infty}^{\infty} J_l^2\left(\frac{k_\perp v_\perp}{\omega_{He}}\right) \\ &\times \int_{-\infty}^{\infty} \frac{dv_z}{\omega - k_z v_z - l\omega_{He}} \left(\frac{l\omega_{He}}{v_\perp} \frac{\partial f_0^e}{\partial v_\perp} + k_z \frac{\partial f_0^e}{\partial v_z} \right) = 0, \\ \mathbf{v} &= \mathbf{v}(v_\perp, \theta, v_z); \\ \varphi(\mathbf{r}, t) &= \int_{-\infty}^{\infty} d\mathbf{k} \varphi_{\mathbf{k}} \exp\{i(\mathbf{k}\mathbf{r} - \omega_{\mathbf{k}}t)\}, \\ \varphi_{\mathbf{k}}^* &= \varphi_{-\mathbf{k}}, \quad \omega_{\mathbf{k}} = -\omega_{-\mathbf{k}}. \end{aligned} \quad (1)$$

Here $\omega_{p\mu}^2 = 4\pi ne^2/m_\mu$ (μ is the particle species),

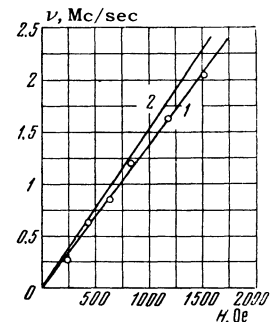
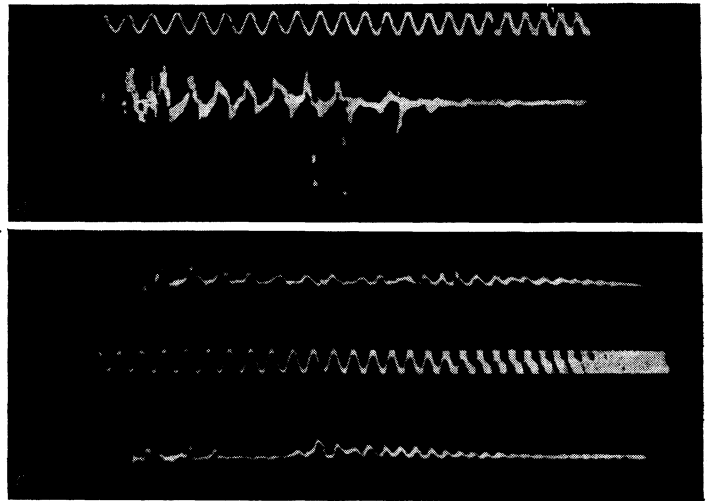


FIG. 15. The frequency of the fundamental in the plasma noise as a function of the strength of the fixed magnetic field in the trap (curve 1). The frequency of the fundamental is close to the ion-cyclotron frequency for protons (curve 2).

FIG. 16. Oscillograms of the readings of the double electric probe. a) The current oscillations correspond to free magnetoacoustic oscillations of the plasma column at a frequency close to the circuit frequency; b) in the second half of the current oscillogram there are oscillations at a higher frequency corresponding to another mode. The period of the calibrating signal is $0.09 \mu\text{sec}$; $H_z = 500 \text{ Oe}$, $H = 1300 \text{ Oe}$, $n \approx 2 \times 10^{12} \text{ cm}^{-3}$.



$\omega_{\text{He}} = eH/mc$, and the remaining notation is conventional. Equation (1) and all the following equations are written in the coordinate system in which the electrons are at rest and in which the ions move with velocity \mathbf{u} across the magnetic field H_z . The effect of the magnetic field on the ion motion in the wave is neglected and it is also assumed that the ions are cold.

It should be emphasized that Eq. (1) is derived under the assumption that the zero-order distribution function $f_0(v)$ (on which the oscillations occur) is stationary and uniform. In the present case the zero-order quantities depend on coordinates and time. This situation can be neglected only for high-frequency oscillations and small wavelengths.

Equation (1) can be investigated in two limiting cases: $k\rho_{\text{He}} \gg 1$ and $k\rho_{\text{He}} \ll 1$, where ρ_{He} is the electron Larmor radius. In the first case Eq. (1) is written in the form

$$\varepsilon(\omega, \mathbf{k}) \equiv 1 - \frac{\omega_{pi}^2}{(\omega + \mathbf{k}\mathbf{u})^2} + \frac{\omega_{pe}^2}{k} \int_{-\infty}^{\infty} \frac{dv}{\omega - kv} \frac{\partial f_0^e}{\partial v} = 0. \quad (2)$$

An investigation of the dispersion relation (1) for the case $k\rho_{\text{He}} \ll 1$ shows that the most unstable oscillations are those for which

$$(u/c_e)^2 \gg (k_z/k)^2 \gg (u/c_e)^2 (k\rho_{\text{He}})^2,$$

where c_e is the mean thermal velocity of the electrons. In this range of values of k_z/k the dispersion equation for the long wave oscillations is the same as Eq. (2) if k is replaced by k_z in the integral:

$$\varepsilon(\omega, k) \equiv 1 - \frac{\omega_{pi}^2}{(\omega + ku)^2} + \frac{\omega_{pe}^2}{k^2} k_z \int_{-\infty}^{\infty} \frac{dv_z}{\omega - k_z v_z} \frac{\partial f}{\partial v_z} = 0. \quad (3)$$

As long as the oscillation amplitude is small

the growth in time is exponential and each mode grows independently of the others. At higher amplitudes the nonlinear interaction between modes characterized by different \mathbf{k} becomes important and this interaction acts to limit the further growth of the unstable modes. Nonlinear processes lead to an exchange of energy between modes in the spectral range of unstable \mathbf{k} , including values of \mathbf{k} for which the oscillations are absorbed by Landau damping; this phenomenon causes plasma heating.¹⁾

The wave kinetics can be treated using the example of a one-dimensional oscillation spectrum (\mathbf{k} parallel to \mathbf{u}). In the range of values of \mathbf{k} in which the oscillations are stable and $\omega_{pe}/c_e \gg k \gg 1/\rho_{\text{He}}$ the spectral density of the oscillation energy w_k is determined from the kinetic equation for the "mode occupation numbers" N_k :^[8]

$$\begin{aligned} \frac{dN_{k\alpha}}{dt} = & 2\nu_{k\alpha}N_{k\alpha} + \pi \sum_{\beta\gamma} \iint dk' dk'' \delta(k' + k'' - k) \\ & \times \delta(\omega_{k\alpha} - \omega_{k'\beta} - \omega_{k''\gamma}) W(\omega_{k\alpha}, \omega_{k'\beta}, \omega_{k''\gamma}) \\ & \times (N_{k'\beta}N_{k''\gamma} - N_{k\alpha}N_{k'\beta} - N_{k\alpha}N_{k''\gamma}) \\ & + 2 \sum_{\beta\gamma} \iint dk' dk'' \delta(k' + k'' - k) \\ & \times \text{Im P} \left[\frac{1}{\varepsilon(\omega_{k\alpha} - \omega_{k'\beta})} \frac{\partial}{\partial \omega} \varepsilon(\omega_{k\alpha} - \omega_{k'\beta}) \right. \\ & \left. \times W(\omega_{k\alpha} - \omega_{k'\beta}, \omega_{k\alpha}, \omega_{k'\beta}) \right] N_{k\alpha}N_{k'\beta}, \end{aligned} \quad (4)$$

¹⁾By heating we mean an increase in the mean particle energy

$$\frac{m_\mu}{2} \int (v - \mathbf{u})^2 f_\mu dv.$$

We shall call this the "temperature" and denote it by the expression $T_\mu = \frac{1}{2} m_\mu c_\mu^2$.

$$W(\omega_{k\alpha}, \omega_{k'\beta}, \omega_{k''\gamma}) = \left[\frac{\partial \varepsilon}{\partial \omega_{k\alpha}} \frac{\partial \varepsilon}{\partial \omega_{k'\beta}} \frac{\partial \varepsilon}{\partial \omega_{k''\gamma}} \right]^{-1} \\ \times \left[\sum_{\mu} \frac{4\pi e^3}{m_{\mu}^2} \int dv \frac{\partial f_0^{\mu} / \partial v}{(\omega_{k\alpha} - kv)(\omega_{k'\beta} - k'v)(\omega_{k''\gamma} - k''v)} \right]^2.$$

(The subscripts α, β, γ denote branches of the oscillations and assume the values 1, 2, 3 for the spectrum derived below (6).) The mode occupation number N_k is related to the energy density w_k by

$$w_k \equiv \frac{1}{8\pi} k^2 \frac{\partial}{\partial \omega_k} \omega_k \varepsilon(\omega_k) |\Phi_k|^2 = N_k \omega_k.$$

We now examine the meaning of the terms in Eq. (4). The first term on the right side takes account of the production or absorption of modes characterized by wave vector k . In particular it includes the linear Landau damping. The second term describes the change in the mode occupation number as a result of processes with the participation of three waves with different k : decay of modes with wave vector k into two modes k' and k'' and also the inverse process of fusion and scattering of the type $k + k' = k''$. In these processes energy and momentum are both conserved. For example, in mode decay

$$k = k' + k'', \quad \omega_{k\alpha} = \omega_{k'\beta} + \omega_{k''\gamma}.$$

The change in the total energy of the interacting mode is associated with processes described by the third term. It takes account of processes in which the combination of two modes with frequencies $\omega_{k\alpha}$ and $\omega_{k'\beta}$ forms modes characterized by frequencies $\omega_{k''} = \omega_{k\alpha} - \omega_{k'\beta}$ where $k'' = k - k'$ and these modes are absorbed by resonance particles, for which $v = \omega_{k''}/k''$. Hence this process is essentially a nonlinear Landau damping effect. Although the nonlinear Landau damping is formally small compared with the term $2\nu_k N_{k\alpha}$, it is important for waves in which the linear damping is small or completely absent.

Landau damping due to resonance particles leads to a change in the zero-order distribution function.^[9] This process is described by the quasilinear equation for the electron and ions

$$\frac{\partial f_0^{\mu}}{\partial t} + \frac{\partial}{\partial v} 8\pi^2 \frac{e^2}{m_{\mu}^2} \sum_{\alpha} \int dk \frac{N_{k\alpha}}{\partial \varepsilon / \partial \omega_{k\alpha}} \delta(\omega_{k\alpha} - kv) \\ \times \frac{\partial f_0^{\mu}}{\partial v} - \dot{u} \frac{\partial f_0^{\mu}}{\partial v} - \frac{e_{\mu}}{m_{\mu}} [\mathbf{vH}] \frac{\partial f_0}{\partial v} = 0. \quad (5)^*$$

Resonance particles which absorb energy diffuse in velocity space v as long as a plateau $\partial f_0^{\mu} / \partial v = 0$ is not formed on the zero-order distribution

function. The position and width of the plateau Δv corresponds to the range of phase velocity $\Delta(\omega/k)$ satisfying the mode spectrum.

We now apply the general considerations given in Eqs. (1)–(5) to the problem of turbulence heating of a plasma. Before proceeding to a detailed analysis of the problem we note some of the salient features of the current instability. The relation given in (2) has been studied quite thoroughly^[10] for a Maxwellian electron distribution function. If the current-associated velocity u is smaller than the thermal velocity of the electrons c_e the resonance electrons excite oscillations with phase velocity $\omega/k \sim (T_e/M)^{1/2}$ (ion acoustic wave). The growth rate for this instability $\nu \sim (\omega^2/k) \partial f_0^e / \partial v$. When $u > u^* \sim c_e$ a hydrodynamic instability is excited and the growth rate is independent of the detailed structure of the distribution function as in the case $u < u^*$, but is determined by the amount by which the current-associated velocity u exceeds the critical velocity u^* . It increases with increasing $u - u^*$ and k and reaches a maximum value $\nu_m \sim (m/M)^{1/3} \omega_{pe}$ when $k \sim u/\omega_{pe}$.

Since Eqs. (2) and (3) have the same structure it is easy to establish the nature of the instability for long-wave oscillations $k\rho_{He} \ll 1$. The hydrodynamic instability now also exists when $u < u^*$. The instability arises for waves for which $k_z < k \cdot u/u^*$

$$\nu_{max} \sim (m/M)^{1/3} (k^2 k_z c_e^3)^{1/3} \ll (mu/Mc_e)^{1/3} \omega_{He}.$$

In order to facilitate the analysis of nonlinear processes associated with current instability we first consider the case in which the magnetic field is such that the amplitude of the long waves cannot increase appreciably while the rf circuit is in operation. We then estimate the contribution in the electron heating due to long waves.

Assume that the plasma heating process is determined by short waves $k\rho_{He} \gg 1$. We have already estimated the maximum growth rate $\nu_m \sim (m/M)^{1/3} \omega_{pe}$. In a plasma with density $n > 10^{13} \text{ cm}^{-3}$ the quantity $\nu u/\dot{u} > 10^2$. Thus, in the heating process at each instant of time there will be established some spectral distribution of waves N_k which varies slowly with increasing current-associated velocity $u(t)$. If

$$N_k \gg \frac{nT_e}{\omega_{pe}^2} \frac{\partial \varepsilon}{\partial \omega} \frac{\partial \omega}{dk} \frac{\dot{u}}{u},$$

it follows from Eq. (5) that there will always be a plateau on the distribution function $\partial f_0^{\mu} / \partial v = 0$ in the velocity range Δv in which the phase veloci-

* $[\mathbf{vH}] = \mathbf{v} \times \mathbf{H}$

ties of the steady-state oscillations appear. Hence, in Eq. (2) the integral is to be computed in the sense of the principal value. This means that ion acoustic waves are not excited in this regime; the only waves that are excited correspond to a hydrodynamic instability for $u > u^* \sim c_e$.

As the current velocity increases the quantity $u - u^*$ increases. On the other hand, the non-linear damping of oscillations, which leads to plasma heating, reduces this quantity. The steady state supercritical equilibrium must then obviously be determined by the value of the parameter $\nu_m u/\dot{u}$ and occurs at slight "supercriticality" when $\nu_m u/\dot{u} \gg 1$. In a weakly supercritical regime waves are excited which propagate almost parallel to the current with phase velocity of order $c_e (m/M)^{1/3}$. The stability limit is determined by an integral condition on the distribution function

$$I(u, c_e) \equiv c_e^2 \int \frac{\partial f_0^e / \partial v}{u + v} dv = 0.$$

For a Maxwellian function $f_0^e \sim \exp(-m\nu^2/2T_e)$ this condition is satisfied when $u \approx -0.9 c_e$. The spectrum of electron-ion oscillations in the vicinity of unstable values of \mathbf{k} is of the form

$$\begin{aligned} \omega_{1,2} &= -\mathbf{k}\mathbf{u} + \eta k c_e \pm \left(\frac{2}{3I_u} \eta \right)^{1/2} (k^2 - k_0^2)^{1/2} \frac{c_e}{\omega_{pe}}, \\ \omega_3 &= -\mathbf{k}\mathbf{u} - \frac{1}{2} \eta k c_e, \\ k_0^2 &= \frac{\omega_{pe}^2}{c_e^2} \left\{ I + I' \left[\eta - \left(1 - \frac{\mathbf{k}\mathbf{u}}{ku} \right) \right] \right\}, \\ \eta &= \left(\frac{2}{I_u} \frac{m}{M} \right)^{1/3}, \quad I_u \sim -1. \end{aligned} \quad (6)$$

The relation in (6) can be applied for values of \mathbf{k} that are not too large, in which case $k^2 < (\omega_{pe}/c_e)^2 \eta$. The limiting value k_0 and consequently, the growth rate of the instability ν_k , are determined by the parameters of the steady-state turbulence heating regime (the electron temperature T_e , the density n and the quantity \dot{u}/u).

We now consider the kinetics of waves described by Eq. (4). The spectral distribution of the oscillations N_k for $k > k_0$ is determined by three processes: the influx of oscillation energy from the range $k < k_0$ where the oscillation "sources" are located, the loss of energy as a consequence of nonlinear Landau damping, and loss due to decay processes. In the steady-state regime the influx of oscillation energy must be balanced by the non-linear damping.

The effect of linear electron Landau damping

on the wave kinetics is insignificant in the present experiment. The diffusion process in v -space, which is described by the nonlinear term in Eq. (5) for the electrons, leads to the establishment of a plateau. The relative width of the plateau is small:

$$\Delta v/c_e = \Delta(\omega/k)/c_e \sim (m/M)^{1/2}.$$

As a result of the establishment of the plateau the electron temperature increases by an amount $\Delta T_e \sim T_e (\Delta v/c_e)^3 \sim T_e (m/M)^{2/3}$. As the current-associated velocity increases, the width of the plateau increases slowly. However, during the turbulence-heating process the electron temperature must increase at a rate $\dot{T}_e \sim 1/2 m \dot{u}^2$. Hence the small contribution to the temperature change due to the increase in the plateau can be neglected. It is evident that in the overall energy balance one need not take account of the energy loss due to the increase in the plateau width, i.e., the linear Landau damping.

Comparing the second and third terms in Eq. (4) it is evident that the wave interaction process for the spectrum in Eq. (6) goes approximately $(M/m)^{1/3}$ times faster than the nonlinear Landau damping process and equilibrates it to the influx of oscillation energy from the region $k < k_0$. Hence, in the zeroth approximation the spectral distribution of the modes should be determined by decay processes which lead to the establishment on branches 1 and 2 of a Rayleigh-Jeans distribution for the mode occupation number $N_{k\alpha} = (nc_e/\omega_{pe}) \Theta / \omega_{k\alpha}$, where Θ is the wave temperature.

The temperature of the waves can be determined as follows: in the quasistationary regime, in which $u(t) = u^*(t) \sim c_e(t)$ during the entire process, the rate of electron heating \dot{T}_e is due to the absorption by the electrons of oscillations at temperature Θ from branches 1 and 2 as a consequence of nonlinear Landau damping:

$$\Theta \sim T_e (\omega_{pe} u/\dot{u})^{-1/2}. \quad (7)$$

The current-driven instability can heat the ions as well as the electrons. An investigation of the dispersion equation (2) shows that when \mathbf{k} is of order ω_{pe}/c_e the frequencies $\omega_{2,3}$ approach the ion plasma frequency. Consequently the phase velocity of these oscillations can be of the order of the ion thermal velocity. Strong linear Landau damping of these oscillations should lead to ion heating at a rate that can be estimated from Eq. (5) written for the ions. The diffusion process in v -space, which is unimportant for the electrons, leads to ion heating at a rate

$$\dot{T}_i \sim T_e (m/M)^{1/2} (\omega_{pe} u / \dot{u})^{-1/2}. \quad (8)$$

The ion-heating rate becomes equal to the electron-heating rate when $(\omega_{pe} u / \dot{u}) m/M \gtrsim 1$. We emphasize that the heating process described here can be established only during the course of a monotonic rise in current-associated velocity.

We now estimate the contribution to electron heating for wavelength $k\rho_{He} \ll 1$. It follows from Eq. (3) that the critical velocity for the long-wave hydrodynamic instability is of the order of the ion thermal velocity. Hence, in contrast with the case $k\rho_{He} \gg 1$, electron heating due to nonlinear Landau damping does not lead to the appearance of a long-wave instability. In the strongly supercritical regime the most unstable perturbation grow almost a periodically with growth rate $\gamma \sim \omega \sim (\mu/Mc_e)^{1/3} \omega_{He}$. To estimate the electron heating rate due to the absorption of these oscillations we again use Eq. (4), although the application of this equation in an essentially aperiodic case is open to question. The calculations give

$$\dot{T}_e \sim T_e \omega_{He} (u/c_e)^3 (m/M)^{1/2}. \quad (9)$$

The long-wave instability and the electron heating associated with it are specially important when $u < c_e$, in which case the short waves are stable.

To compare the theory given here with experiment one must know how the current-associated velocity u is related to the measured parameters of the rf circuit and the plasma. In the general case of a nonlinear highly damped hydromagnetic wave it is difficult to establish this relation. In [2] the two simplest situations were considered: the case of quasistationary compression of the plasma by the alternating magnetic field and the case of small wave amplitudes. The current-associated velocity in a plane wave $(H_\sim)_z = H_\sim \sin(k_z r - \Omega t)$, which propagates across the magnetic field H , $H_\sim/H \ll 1$, is given by the expression

$$\frac{\mu u^2}{2} = \frac{H_\sim^2}{8\pi n} \frac{\Omega^2}{|\omega_{i,e}^2 - \Omega^2|}, \quad \omega_{i,e}^2 = \frac{e^2 H^2}{m M c^2}. \quad (10)$$

The kinetic energy of the electrons in the current-associated motion $\mu u^2/2$ has a peak at $\bar{H} = (\Omega^2 m M c^2 / e^2)^{1/2}$ and falls off as H^{-2} as H increases. At smaller values of H the wave field penetrates into the plasma only to a skin depth c/ω_{pe} .

The value of H is small at the circuit frequency $\Omega/2\pi = 10^7$ and is approximately 150 Oe for protons. For appreciable heating of a plasma with densities 10^{12} – 10^{13} one requires an alternating field value comparable with or greater than \bar{H} . Hence the majority of the present measure-

ments were carried out at $H_\sim/H \sim 1$ in which case Eq. (10) only applies qualitatively. Actually, as a consequence of the curvature of the front of the highly nonlinear hydromagnetic wave the quantity $\mu u^2/2$ must be larger than given by Eq. (10) and its dependence on field in some range of values of H must be weaker.

As we have shown above, because of the current-associated instability the temperature of the plasma electrons at each instant of time must be greater than $\mu u^2/2$. Hence the energy absorbed by the plasma must depend on the field H in the same way as $\mu u^2/2$ while the maximum effective heating $8\pi n T_e / H^2$ must be of order unity. These theoretical conclusions are qualitatively verified by the measured dependence of energy absorbed from the circuit described in [2] and the measured dependence of electron temperature T_e in turbulence heating on the plasma density n .

The maximum heating efficiency $8\pi n T_e / H_\sim^2$ for a fixed value of $H_\sim^2/8\pi$ must depend only on circuit parameters so that a change in plasma density means that the pressure must remain fixed. In Fig. 17 we have plotted the quantities n_e and T_e as measured by three different methods: by bremsstrahlung in the region of large values of T_e and small n , and by the optical method and the probe method at high densities. All the experimental points give satisfactory agreement with the line $n T_e \approx 10^{15}$ eV cm⁻³. These measurements were carried out at alternating fields of $H_\sim = 500$ Oe so that $8\pi n T_e / H_\sim^2 = 0.2$.

Ion heating has been observed in these experiments. This effect can be explained by the theory given here. Ion heating is possible if $(\omega_{pe} u / \dot{u}) m/M \gtrsim 1$ and this condition is satisfied in the present experiments.

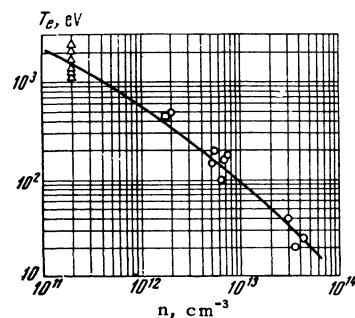


FIG. 17. The electron temperature T_e as a function of plasma density n in turbulence heating $H_\sim = 500$ Oe, $H = 500$ Oe. (○) data obtained by the optical method, (△) data obtained by x-ray measurements, (□) mean of the many results obtained by probe measurements. In the region 5×10^{11} cm⁻³ $\leq n \leq 4 \times 10^{13}$ cm⁻³, using the curve we find $n T_e = 10^{15}$ eV·cm⁻³. The value of this product at optimum heating, as indicated by the measurements, is proportional to H_\sim^2 .

We emphasize that the comparison of certain experimental facts given here with the theory that we have proposed indicates primarily that there are no contradictions. In order to make sure that turbulence heating is due to the processes described here it would be desirable to observe the mode spectrum during heating.

7. SUMMARY OF RESULTS

1. A detailed experimental investigation has verified that it is possible to obtain rapid and effective collisionless heating of plasma electrons to high temperatures by means of a strong hydromagnetic wave which propagates across the magnetic field. In the present apparatus we have established that $nT_e \approx 10^{15} \text{ eV cm}^{-3}$ over a wide range of values of the density n .

2. It has been established that under certain conditions the electron heating in the wave is accompanied by appreciable ion heating.

3. We have proposed a mechanism for collisionless heating of electrons and ions in a strong hydromagnetic wave. Qualitative agreement has been shown between the experiments and this theory of turbulence heating.

4. We have investigated the confinement of a plasma heated by turbulence heating in a trap. The confinement time for high-temperature ions in the trap reaches $130 \mu\text{sec}$ when $n = 10^{12} \text{ cm}^{-3}$. The confinement time for hot electrons is $60 \mu\text{sec}$ when $n = 10^{12} \text{ cm}^{-3}$, in approximate agreement with the escape of electrons by virtue of collisions. During this time period no strong instabilities are observed in the plasma which could lead to the rapid loss of plasma.

5. Strong ion-cyclotron waves are observed in the plasma. With certain choices of the values of density and magnetic field strong oscillations of the plasma column are excited. These oscillations evidently correspond to magnetic-sound resonance of the plasma at the frequency of the rf circuit.

¹ Babykin, Zavoiskii, Rudakov, and Skoryupin, Nuclear Fusion, Supp. 3, 1962.

² Babykin, Gavrin, Zavoiskii, Rudakov, and Skoryupin, JETP 43, 411 (1962), Soviet Phys. JETP 16, 295 (1963).

³ Babykin, Gavrin, Zavoiskii, Rudakov, and Skoryupin, JETP 43, 1547 (1962), Soviet Phys. JETP 16, 1092 (1963).

⁴ Babykin, Zavoiskii, Rudakov, and Skoryupin, JETP 43, 1976 (1962), Soviet Phys. JETP 16, 1391 (1963).

⁵ Bulyginskiĭ, Galaktionov, Dolmatova, and Ovsyannikov, ZhTF 33, 183 (1963), Soviet Phys. Tech. Physics 8, 131 (1963).

⁶ Zagorodnikov, Smolkin, and Sholin, JETP 45, 1850 (1963), Soviet Phys. JETP 18, 000 (1964).

⁷ E. G. Harris, Phys. Rev. Letters 2, 34 (1959).

⁸ V. I. Karpman, DAN 152, 587 (1963), Soviet Phys. Doklady 8, 919 (1964).

⁹ A. A. Vedenov, Atomnaya Énergiya 13, 5 (1962).

¹⁰ I. B. Bernstein, Nuclear Fusion 1, 65 (1960).

Translated by H. Lashinsky